Theor Chem Acc (2012) 131:1238
DOI 10.1007/s00214-012-1238-3

REGULAR ARTICLE

# Ruthenocene and cyclopentadienyl pyrrolyl ruthenium as precursors for ruthenium atomic layer deposition: a comparative study of dissociation enthalpies

**Quan Manh Phung · Steven Vancoillie · Annelies Delabie · Geoffrey Pourtois · Kristine Pierloot**

Received: 2 March 2012 / Accepted: 14 May 2012 / Published online: 20 June 2012


**Abstract** $RuCp_2$ (ruthenocene) and RuCpPy (cyclopentadienyl pyrrolyl ruthenium) complexes are used in ruthenium (Ru) atomic layer deposition (ALD) but exhibit a markedly different reactivity with respect to the substrate and co-reactant. In search of an explanation, we report here the results of a comparative study of the heterolytic and homolytic dissociation enthalpy of these two ruthenium complexes, making use of either density functional theory (DFT) or multiconfigurational perturbation theory (CASPT2). While both methods predict distinctly different absolute dissociation enthalpies, they agree on the relative values between both molecules. A reduced heterolytic dissociation enthalpy is obtained for RuCpPy compared to $RuCp_2$, although the difference obtained from CASPT2 (19.9 kcal/mol) is slightly larger than the one obtained with any of the DFT functionals (around 17 kcal/mol). Both methods also agree on the more pronounced stability of the $Cp^-$ ligand in RuCpPy than in $RuCp_2$ (by around 9 kcal/mol with DFT and by 6 kcal/mol with CASPT2).

**Keywords** Ruthenocene · Dissociation enthalpy · DFT · CASPT2

## 1 Introduction

Atomic layer deposition (ALD) [1] is an advanced technique to deposit nanometer-thin films on a substrate, starting from gas-phase precursors and making use of a cyclic process of at least two consecutive self-limiting chemisorption reactions, the so-called "reaction cycle". Two important properties, namely (a) conformal deposition on complex nanostructures (i.e., following the shape of the underlying structure) and (b) control of the deposition process at the atomic level, have turned ALD into a powerful technique in nanotechnology [2]. For example, ALD is used in the industrial production of MOSFETs (Metal Oxide Semiconductor Field Effect Transistors) and memories to deposit thin highly insulating dielectric oxide layers [3].

ALD of ruthenium (Ru) is currently under extensive investigation. Ru is a new electrode material for trenched metal–insulator–metal capacitors of dynamic random access memories (DRAM), as well as a possible component of the metal connection between the elements of an integrated circuit. The Ru ALD reaction cycle consists of two reactions: a Ru precursor chemisorption reaction followed by a co-reactant chemisorption reaction. The most suitable precursors for ALD of high-quality Ru thin films have not yet been identified. Ru precursors under investigation are the organometallic Ru compounds with cyclopentadienyl (Cp, $C_5H_5$) or pyrrolyl (Py, $C_4H_4N$) ligands,

Published as part of the special collection of articles celebrating theoretical and computational chemistry in Belgium.

**Electronic supplementary material** The online version of this article (doi:10.1007/s00214-012-1238-3) contains supplementary material, which is available to authorized users.

Q. M. Phung · S. Vancoillie (✉) · K. Pierloot
Department of Chemistry, University of Leuven, Celestijnenlaan 200F, 3001 Leuven, Belgium
e-mail: steven.vancoillie@chem.kuleuven.be

A. Delabie · G. Pourtois
imec, Kapeldreef 75, 3001 Leuven, Belgium

G. Pourtois
Department of Chemistry, PLASMANT research group, University of Antwerp, Universiteitsplein 1, 2619 Antwerp, Wilrijk, Belgium

$\beta$-diketonates, amidinates, and $RuO_4$ [4, 5]. An ALD precursor should be stable in the gas phase, but reactive on both the initial substrate and the deposited film. $RuCp_2$ and RuCpPy as well as their substituted complexes, for example, $Ru(EtCp)_2$ (Et = ethyl) and Ru(MeCp)Py (Me = methyl), have the advantage to be stable up to high temperatures in the gas phase and may be used in combination with different co-reactants, such as $O_2$ or a plasma ($N_2$, $H_2$, $N_2/H_2$, or $NH_3$ plasma). In the latter case, the process is referred to as plasma-enhanced ALD or PEALD (Fig. 1). In a recent comparative study of $Ru(EtCp)_2$ and Ru(MeCp)Py as precursors for PEALD of Ru, the reactivity of these two molecules was found to be quite different [6]. Starting from a TiN surface, a major nucleation delay was observed for the $Ru(EtCp)_2$ precursor, whereas much better nucleation was observed with Ru(MeCp)Py. Moreover, the growth-per-cycle at steady state, that is, the thickness of the deposited Ru layer per reaction cycle, was 0.038 nm/cycle for Ru(MeCp)Py, but only 0.016 nm/cycle for $Ru(EtCp)_2$.

Fundamental understanding of ruthenium ALD chemisorption reaction mechanisms and how the precursor chemistry controls the process (e.g., the specific role of Py versus Cp ligands) is still lacking. Theoretical calculations may play an important role in obtaining such understanding, by providing information concerning the stability of different ALD precursors and by predicting possible chemisorption reaction mechanisms. However, so far, almost no theoretical studies of reaction mechanisms for Ru ALD have been reported in the literature. Only one study reports the reaction mechanisms for homoleptic Ru precursors and oxygen [7]. In this work, we present the results from a computational study of the relative stability of $RuCp_2$ and RuCpPy with respect to ligand dissociation, either heterolytically or homolytically. No substituents on the ligands were included, as experiments have indicated that such substituents only have a minor influence on the ALD process. We have employed both density functional theory (DFT) and multiconfigurational perturbation theory (CASPT2) to obtain the Ru–Cp and Ru–Py binding energies. No experimental data are available for the dissociation enthalpies of the complexes studied. Therefore, to judge the quality of the present calculations, we will rely on the results of our previous computational study [8], using the same approach, of the heterolytic dissociation enthalpy of a number series of first-row metallocenes $MCp_2$ (M = V, Mn, Fe, Ni) for which experimental data are indeed available. In that study, we showed that with multiconfigurational perturbation theory, CASPT2 or RASPT2 (with "R" denoting that the reference wave function is built from a restricted rather than a complete active space) based on an extended active space (up to 18 active orbitals), the dissociation enthalpy of these first-row metallocenes may be predicted with an accuracy that is close to (or even within) the experimental accuracy for manganocene, ferrocene, and nickelocene (the difference with the experimental values amounting to 0.5, 4.1 and −6.6 kcal/mol, respectively), while a (unexpected) larger error, 9.6 kcal/mol, was obtained for vanadocene. Of course, since we have no experimental values for the dissociation enthalpies of ruthenocene, we can never be completely sure that the CASPT2 errors are similar to those of the first-row metallocenes. Among the DFT functionals used, the hybrid functional B3LYP-D is obviously superior, with an average (absolute) error on the dissociation enthalpy of 4.1 kcal/mol and a maximum error of +8.7 kcal/mol for nickelocene. Importantly, both dispersion interactions and relativistic effects were found to give significant contributions to the binding energies, and should therefore be taken into account. Two other functionals, PBE0 and M06, were also intensively studied, but were both found to overbind, with average errors of +12.4 kcal/mol (PBE0, with dispersion corrections taken from B3LYP) and 11.3 kcal/mol (M06). In this work, we will present the results obtained from DFT with three functionals, that is, the hybrid functionals B3LYP and PBE0 and the GGA PBE. The latter functional is included because it is widely used in solid-state calculations, an alternative approach to study the bonding and reactivity of the present Ru compounds at different surfaces, which we intend to use in a future study. The main goal of the present study therefore is to benchmark the results obtained with different functionals, PBE in particular, against high-level ab initio results.

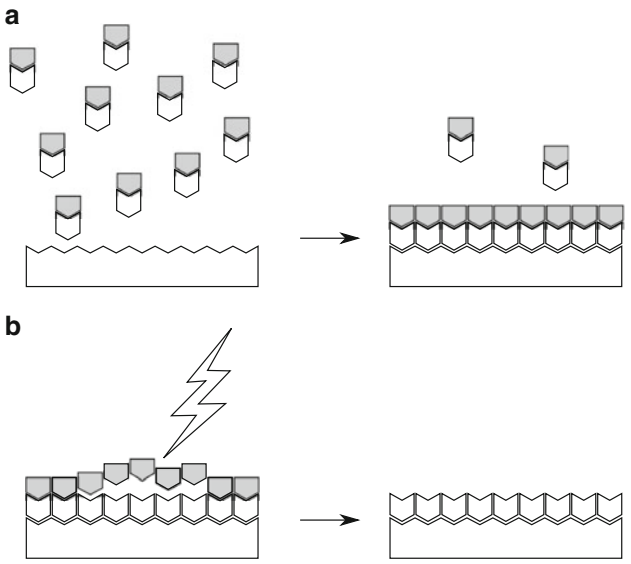


**Fig. 1** Schematic representation of the reaction cycle for Ru PEALD. **a** Ru precursor chemisorption reaction, **b** plasma reaction

## 2 Computational details

Both density functional theory (DFT) and multiconfigurational perturbation theory, that is, complete active space self-consistent field (CASSCF) followed by second-order perturbation theory (CASPT2), were used to investigate the heterolytic and homolytic dissociation enthalpies of $RuCp_2$ and RuCpPy. The enthalpies of nine possible reaction steps involved in the dissociation (R1–R9, see Figs. 2, 3) were computed. All DFT calculations were performed with TURBOMOLE v. 6.3 [9], while the CASSCF/CASPT2 calculations were performed with MOLCAS 7.6 [10].

Extensive basis sets were used in the DFT calculations: def2-QZVPP for the Ru atom [11] and def2-TZVP for all other atoms [12]. We showed previously that these basis sets yield reliable results with small basis set superposition errors (BSSE) [8]. To describe scalar relativistic effects, an effective core potential was used for ruthenium, describing the behavior of 28 core electrons (ecp-28-mwb) [13]. A dispersion correction to DFT (DFT-D2) [14] was used to cover the attractive dispersion interaction between two cyclopentadienyl rings, which was shown to contribute significantly to the metal–Cp binding energies in our previous study [8]. Since the DFT-D2 parameters are only available for the B3LYP and PBE functionals, dispersion corrections for the PBE0 functional were adopted from B3LYP-D.

For the multiconfigurational perturbation theory (CASPT2) calculations, extended all-electron ANO-RCC basis sets were used with the following contractions: [10s9p8d6f4g2h] for the Ru atom [15], [8s7p4d3f1g] for carbon and nitrogen [16], and [6s4p3d1f] for hydrogen [17]. We showed that such large basis sets are needed to reduce the basis set superposition errors (BSSE) on the heterolytic dissociation enthalpy of first-row metallocenes to an acceptable level of a few kcal/mol [8, 18]. The Cholesky decomposition technique was used to approximate the two-electron integrals, using a threshold of $10^{-6}$ au [19]. Scalar relativistic effects were included using the standard second-order Douglas–Kroll–Hess Hamiltonian [20–22]. In the perturbation step, the default IPEA shift for the zeroth-order Hamiltonian [23] (0.25 au) was used, and an imaginary level shift [24] of 0.1 au was included to prevent weak intruder states. All valence electrons, including the ruthenium (4s,4p) semi-core electrons, were

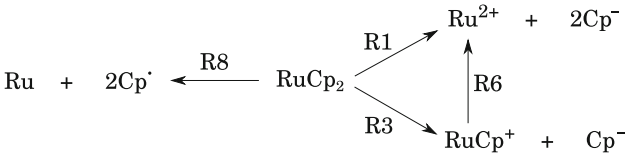


**Fig. 2** Dissociation reactions of $RuCp_2$

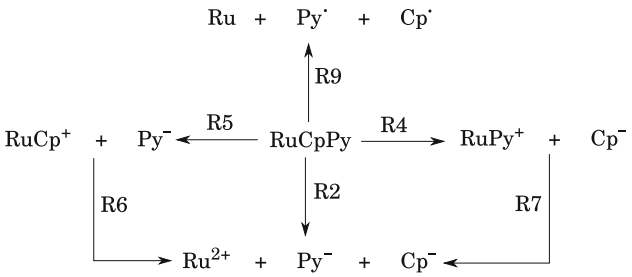


**Fig. 3** Dissociation reactions of RuCpPy

included in the CASPT2 calculations. Since it is computationally unfeasible to optimize the metallocene structure with CASPT2, single-point calculations were instead performed on the ground state PBE0 structures of all molecules. In previous studies [8, 18, 25] we have already shown that this functional performs best for obtaining accurate structures for transition metal complexes (close to experiment, and, in comparison with other functionals, also providing the lowest CASPT2 energy).

Within the $D_{5h}$ symmetry of ruthenocene, the Ru 4d orbitals belong to the irreducible representations (irreps) $a_1'(4d_{z^2}), e_2'(4d_{xy}, 4d_{x^2-y^2})$, and $e_1''$ $(4d_{xz}, 4d_{yz})$, whereas the cyclopentadienyl carbon $2p_z$ orbitals form symmetry-adapted combinations giving rise to six occupied $\pi$ orbitals belonging to the $a_1', a_2'', e_1', e_1''$ irreps, and four empty $\pi^*$ orbitals belonging to the $e_2'$ and $e_2''$ irreps. Only those Cp $\pi$ and $\pi^*$ within the same irreps as the metal d orbitals can interact to form covalent metal–ligand combinations, that is, the $a_1', e_2'$, and $e_1''$ irreps. Since the metal $4d_{z^2}$ and $Cp^-$ $\pi$ orbitals in irrep $a_1'$ are energetically well separated, they do not strongly interact. Ru–Cp bonding occurs through charge donation from the Cp $e_1''$ $(\pi)$ into the metal $e_1''$ $(4d_{xz}, 4d_{yz})$ orbitals, counteracted by backdonation from the metal $e_2'$ $(4d_{xy}, 4d_{x^2-y^2})$ into the Cp $e_2'(\pi^*)$ orbitals. The Cp $e_1''$ $(\pi)$ and $e_2'$ $(\pi^*)$ cyclopentadienyl orbitals should therefore be added to the metal d orbitals in the active space, yielding a total of nine active orbitals containing eight electrons. In previous studies [8, 18], we have shown, however, that a more accurate description of the dissociation enthalpy of metallocenes may be obtained from the second-order perturbation treatment after extending the reference active space with (a) four additional cyclopentadienyl orbitals: $e_1'(\pi)$, $e_2''(\pi^*)$ and (b) an extra virtual 4d′ shell to describe the double-shell effect. This would then give a total of 14 electrons in 18 active orbitals, CAS(14,18) becoming computationally unaffordable with CASSCF. However, test calculations (making instead use of RASSCF, that is, restricting the excitation level in the active space) made clear that an active space of 14 orbitals, lacking two virtual shells $e_1'', e_2'$ would in fact suffice in the present case. The obvious reason is that the nd double-shell effect is much

less pronounced for 4d than for 3d transition metals [26]. This being the case, these four orbitals, which were intended to have Ru 4d′ character, instead rotated into Ru 4f, while remaining very weakly occupied (<0.01). The 14 orbitals included in the CAS(14,14) active space of ruthenocene are plotted in Fig. 4, with their occupation numbers indicated within brackets. As one can see, the weakly occupied $a_1'$ orbital is almost pure $4d'_{z^2}$, whereas the weakly occupied $e_1''(\pi^*)$ shell also shows significant admixture of $(4d'_{xy}, 4d'_{x^2-y^2})$ character. This suffices to describe the 4d double-shell effect in the present $4d^6$ systems.

Upon heterolytic dissociation, the CAS(14,14) active space gets subdivided in a CAS(4,4) space on each of the ligand anions, leaving CAS(10,10) for $RuCp^+$ and $RuPy^+$ and a CAS(6,6) space for the $Ru^{2+}$ ion. In order to provide a more balanced treatment of symmetry and correlation for the $^5D$ ground state of this ion, four extra 4d′ orbitals were included, giving a CAS(6,10) space (note that a similar procedure was also used previously for ferrocene [18]). Using instead the smaller CAS(6,6) space, however, gives a total CASPT2 energy for $Ru^{2+}$, which is lower by only 0.4 kcal/mol, and hence would also lower the CASPT2 results for the heterolytic dissociation enthalpies involving $Ru^{2+}$ (Tables 2, 3) by the same amount. This confirms that the 4d double-shell effect is indeed very limited in the present $4d^6$ case. Homolytic dissociation energies (R8, R9 in Figs. 2, 3) were obtained by subtracting from the heterolytic dissociation energy the $Ru \rightarrow Ru^{2+}$ ionization energy and adding the electron affinities of both ligands. In these calculations, the 4s orbital was included in the active space of the Ru atom, giving CAS(8,11), while the ligand radicals were described with a CAS(3,4) space.

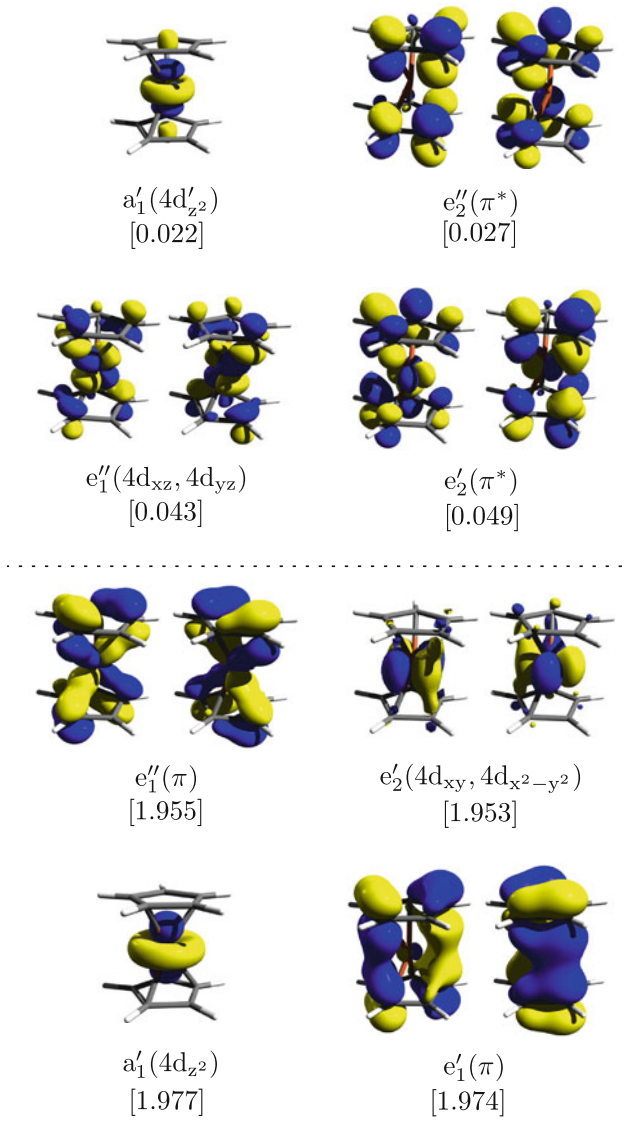


**Fig. 4** The active space CAS(14,14)

Dissociation enthalpies at room temperature $\Delta H^\circ_{298}$ were obtained by starting from the electronic binding energies (denoted as $\Delta E_{elec}$ in Table 2) and including corrections for the zero-point vibrational energy ($\Delta E_{ZPE}$) and thermal energy ($\Delta E_{thermal}$), as obtained from frequency calculations on the molecules involved in the chemical process described. For the CASPT2 data, these values were taken from PBE0. Moreover, a counterpoise correction ($\Delta E_{CPC}$) was added to all binding energies to account for basis set superposition errors. The composition of the dissociation enthalpies $\Delta H^\circ_{298}$ with respect to the different terms described here is provided in Table 2, describing the (full) heterolytic dissociation processes of both considered molecules (reactions R1 and R2). For the other reactions, only $\Delta H^\circ_{298}$ values are given in Tables 3, 4, while the detailed composition of these data is provided in Online Resource 1.

## 3 Results and discussion

### 3.1 Heterolytic dissociation enthalpy of $RuCp_2$ and RuCpPy

Bond distances of the experimental and calculated structures of ruthenocene are shown in Table 1. $RuCp_2$ has an eclipsed structure belonging to the $D_{5h}$ point group, with a $^1A_1'$ electronic ground state. For RuCpPy, the eclipsed geometry ($C_s$ symmetry, $^1A_1'$ electronic state) was also found to be slightly more stable (by 0.3 kcal/mol computed with the B3LYP functional) than the staggered geometry.

GGA functionals are expected to provide reasonably accurate geometries for second-row transition metal complexes [28]. This is true for the PBE functional, giving a Ru–Cp ring distance that is shorter by only 0.013 Å with respect to the experimental value. Corresponding errors of B3LYP and PBE0 are +0.021 Å and −0.021 Å,

**Table 1** Experimental and calculated bond lengths (Å) in $RuCp_2$ and RuCpPy

| | PBE | B3LYP | PBE0 | Exp. [27] |
|---|---|---|---|---|
| $RuCp_2$ | | | | |
| C–C | 1.436(1.437)[a] | 1.427(1.428)[a] | 1.424 | 1.430 |
| Ru–Cp[b] | 1.803(1.794)[a] | 1.837(1.823)[a] | 1.795 | 1.816 |
| RuCpPy | | | | |
| Ru–Cp[b] | 1.797(1.789)[a] | 1.829(1.816)[a] | 1.788 | _ |
| Ru-Py[b] | 1.813(1.805)[a] | 1.850(1.839)[a] | 1.807 | _ |

[a] The values in parentheses correspond to the dispersion corrected geometry

[b] Distance to the center of the ring

respectively. In our previous study on ferrocene [8], the PBE0 geometry of this molecule was found to be in closer agreement with experiment (i.e., shorter by only 0.009 Å). The larger discrepancy observed for the PBE0 functional in case of ruthenocene might arise from the fact that the experimental structure of ruthenocene was measured at 101 K and was not vibrationally corrected [27]. As the values within parentheses in Table 1 indicate, including a dispersion correction leaves the C–C and C–H distances invariant, while shortening the Ru–Cp and Ru–Py ring distances. Obviously, this is related to the attractive dispersion interaction between both ligands, as was also found in first-row metallocenes [8]. All functionals predict a shorter Ru–Cp distance (by about 0.01 Å) in RuCpPy as compared to $RuCp_2$. The Ru–Cp distance is also systematically shorter by 0.02 Å than the Ru–Py distance.

We started by studying the full heterolytic dissociation reactions of both molecules: R1 (Fig. 2) and R2 (Fig. 3). The computed dissociation enthalpies are shown in Table 2. Among the DFT results, we find the following order with respect to the size of the heterolytic dissociation enthalpies: PBE > PBE0 > B3LYP, with differences of around 20 kcal/mol between successive results in this list. The CASPT2 results are in between PBE and PBE0, 9–11 kcal/mol lower than the PBE values, and about 30 kcal/mol higher than the lowest DFT result, obtained from B3LYP. These trends are very similar between both molecules. However, it is already clear from these results that the Ru–Py bond is considerably weaker than the Ru–Cp bond. We can see that the heterolytic dissociation enthalpy of RuCpPy is 17.4, 17.2, and 18.1 kcal/mol smaller than the corresponding value of $RuCp_2$ using PBE, B3LYP, and PBE0 functionals, respectively. Thus, the difference between the data obtained for both molecules remains virtually constant across the different functionals and is also close to the difference obtained with CASPT2, 19.9 kcal/mol.

We note that the DFT results in general show the same general trends as for ferrocene [8], although for the latter molecule, a much larger difference was found between the PBE and PBE0 result of $\Delta H^\circ_{298}$ (60 kcal/mol, as compared to 20 kcal/mol here), whereas the results obtained with both hybrid functionals were closer (with a difference of only 10 rather than 20 kcal/mol). More remarkable though are the relative values as compared to CASPT2. Although the ab initio results for ferrocene were obtained with a larger active space of 18 orbitals (and, for that reason, employing RASPT2 rather than CASPT2), we believe that the accuracy of the present CASPT2(14,14) results should be comparable to the RASPT2(14,18) results for ferrocene. This is because the four extra orbitals in the active space of ferrocene are describing the nd double-shell effect, which is pronounced for 3d metals, but much less for the present 4d systems (see also the Sect. 2). The RASPT2(14,18) result for $\Delta H^\circ_{298}$ of ferrocene, 639.1 kcal/mol, agrees with the experimental value, 635 ± 6 kcal/mol, to within the experimental uncertainty. As such, a similar accuracy may be expected for the CASPT2 results presented in Table 2. However, when it comes to judging the quality of the DFT results against CASPT2, we find that for $RuCp_2$ and RuCpPy, the results obtained from the PBE functional are closest, that is, higher by 9–12 kcal/mol, whereas for ferrocene, the same functional grossly overestimates the

**Table 2** $\Delta H^\circ_{298}$ (kcal/mol) of the full heterolytic dissociation reactions of $RuCp_2$ and RuCpPy

| | $RuCp_2 \longrightarrow Ru^{2+} + 2Cp^-$ (R1) | | | | $RuCpPy \longrightarrow Ru^{2+} + Cp^- + Py^-$ (R2) | | | |
|---|---|---|---|---|---|---|---|---|
| | PBE | B3LYP | PBE0 | CASPT2 | PBE | B3LYP | PBE0 | CASPT2 |
| $\Delta E_{elec}$ | 724.6 | 680.0 | 700.8 | 722.8 | 707.1 | 662.8 | 682.8 | 701.1 |
| $\Delta E_{disp}$ | 8.1 | 10.9 | 10.9[a] | _ | 7.5 | 10.1 | 10.1[a] | _ |
| $\Delta E_{CPC}$ | −5.7 | −5.2 | −4.8 | −4.7 | −5.7 | −5.1 | −4.7 | −3.5 |
| $\Delta E_{ZPE}$ | −7.9 | −8.1 | −8.1 | −8.1[b] | −7.0 | −7.3 | −7.4 | −7.4[b] |
| $\Delta E_{thermal}$ | 1.8 | 1.7 | 1.8 | 1.8[b] | 1.6 | 1.6 | 1.7 | 1.7[b] |
| $\Delta H^\circ_{298}$ | 720.9 | 679.3 | 700.6 | 711.8 | 703.5 | 662.1 | 682.5 | 691.9 |

[a] Dispersion correction taken from B3LYP

[b] Taken from PBE0

dissociation enthalpy, by 50 kcal/mol. On the other hand, both hybrid functionals perform considerably worse than for $FeCp_2$. Whereas the PBE0 value of $\Delta H^{\circ}_{298}$, 639.4 kcal/mol, was in excellent agreement with RASPT2 for ferrocene, it is now about 11 kcal/mol too low. Similarly, the B3LYP value is now 30 kcal/mol below CASPT2 instead of 10 kcal/mol in case of ferrocene. In general, the binding enthalpies predicted from DFT are considerably lowered with respect to CASPT2 when going from ferrocene to the present ruthenium complexes.

As a next step in our study of the stability of $RuCp_2$ and RuCpPy, we also looked at the individual dissociation steps of a single $Cp^-$ and $Py^-$ ligand from either $RuCp_2$ or RuCpPy. The results obtained for the reaction enthalpies of the consecutive single ligand dissociation steps (a first ligand in reactions R3, R4, and R5, and a second ligand in reactions R6 and R7; cf. Figs. 2, 3) are collected in Table 3 and presented graphically in Fig. 5. We first note that both $RuCp^+$ and $RuPy^+$ are characterized by a low-spin S = 0 ground state. The lowest triplet excited state was found at a considerably higher energy relative to the singlet ground state, 24.0–29.0 kcal/mol for $RuCp_2$ and 18.4–24.3 kcal/mol for RuCpPy, with the lowest quintet state at an even higher energy. This then also means that the first ligand dissociation step is spin conserving, whereas the second dissociation step involves a singlet-to-quintet spin flip. This fact may be used to (partially) rationalize the trends observed in the DFT data in Table 3. For the first, spin conserving step, the enthalpies obtained from PBE and PBE0 are close to within 5 kcal/mol, the latter functional systematically giving the highest value. On the other hand, B3LYP predicts significantly (10–15 kcal/mol) weaker Ru–ligand bond strengths. As compared to CASPT2, all three functionals underestimate the dissociation enthalpy, although for PBE0, the difference with CASPT2 is small, between 2 and 5 kcal/mol. As for the second dissociation step, here the difference between PBE and PBE0 is much larger. The pure GGA functional PBE typically

**Table 3** Heterolytic dissociation enthalpy $\Delta H^{\circ}_{298}$ (kcal/mol) of the first dissociation reactions R3, R4, and R5 and the second dissociation reactions R6 and R7

| | PBE | B3LYP | PBE0 | CASPT2 |
|---|---|---|---|---|
| $RuCp_2 \longrightarrow RuCp^+ + Cp^-$ (R3) | 232.5 | 221.7 | 236.6 | 241.7 |
| $RuCpPy \longrightarrow RuPy^+ + Cp^-$ (R4) | 241.6 | 231.5 | 245.7 | 247.3 |
| $RuCpPy \longrightarrow RuCp^+ + Py^-$ (R5) | 215.0 | 204.5 | 218.4 | 221.9 |
| $RuCp^+ \longrightarrow Ru^{2+} + Cp^-$ (R6) | 488.4 | 457.6 | 464.0 | 470.1 |
| $RuPy^+ \longrightarrow Ru^{2+} + Py^-$ (R7) | 461.9 | 430.6 | 436.8 | 444.6 |

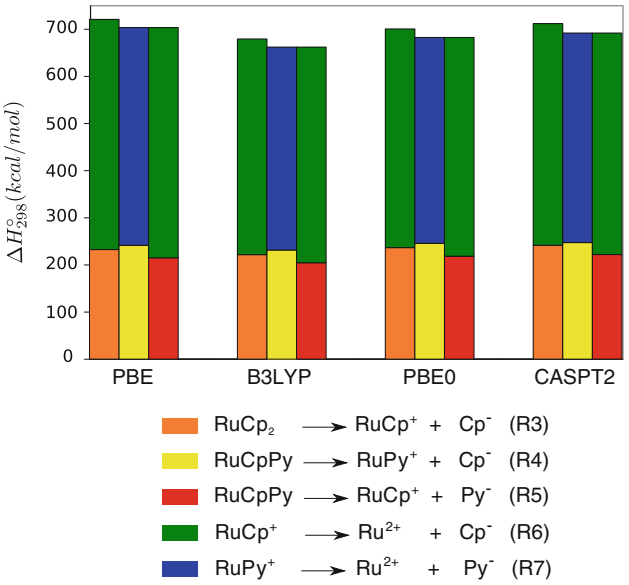


**Fig. 5** Heterolytic dissociation enthalpies of the two consecutive reactions leading to full dissociation of $RuCp_2$ and RuCpPy, as computed with different methods

considerably overestimates the stability of the low-spin monoligated complex with respect to the high-spin $Ru^{2+}$ ground state, thus giving too large binding enthalpies. Including (25 %) Hartree–Fock exchange in PBE0 remediates for this, but seems to overshoot, as the PBE0 binding enthalpies now become smaller by about 7 kcal/mol than the corresponding CASPT2 data. With 20 % Hartree–Fock exchange, B3LYP should do well for the spin flip contribution, but also here this functional seems to quite strongly underestimate the bond strength, by 12–14 kcal/mol as compared to the CASPT2 results.

As Table 3 indicates, both DFT and CASPT2 predict easier dissociation of a first ligand from RuPyCp than from $RuCp_2$. The first ligand to dissociate from RuPyCp is $Py^-$ (R5), and this dissociation step requires 17–18 kcal/mol less with DFT and 19.8 kcal/mol less with CASPT2 than the dissociation of the first $Cp^-$ ligand from $RuCp_2$ (R3). As both reactions result in the same monoligated complex, $RuCp^+$, the differences between the first dissociation enthalpies necessarily equal the differences in the total heterolytic dissociation enthalpies of both molecules (Table 2). Reactions R3 and R4 involve the dissociation of a $Cp^-$ ligand from either $RuCp_2$ or RuCpPy. Comparing these two reactions, we note that the presence of a pyrrolyl rather than a cyclopentadienyl as the second ligand in the complex induces a Ru–Cp bond strengthening: $Cp^-$ dissociation from RuCpPy is harder than from $RuCp_2$ at all calculated levels. This is in agreement with the shorter Ru–Cp ring distance found for the former compound (Table 1). The difference between both dissociation

enthalpies is similar for the different functionals (9.1–9.8 kcal/mol), whereas from CASPT2, a smaller difference of 5.6 kcal/mol is obtained. Reactions R4 and R5 describe the dissociation of either $Cp^-$ or $Py^-$ from RuCpPy. The latter process is clearly more favorable, with a dissociation enthalpy that is lower by as much as 27 kcal/mol with DFT (again fluctuations between different functionals are minor) and slightly less, 25.4 kcal/mol, with CASPT2.

Another important point to note from Table 3 is that the second dissociation steps, either $RuCp^+ \longrightarrow Ru^{2+} + Cp^-$ (R6) or $RuPy^+ \longrightarrow Ru^{2+} + Py^-$ (R7), require an energy which is about twice as high as any of the first dissociation steps. This is another observation that might be relevant to the course of the chemical reactions occurring during the ruthenium ALD process. Indeed, based on this, one might suspect that perhaps a first but not both ligands could be dissociated from the Ru precursor already during the first chemisorption step of the ALD reaction cycle (Fig. 1), meaning that the co-reactant would have to assist in the removal of the second ligand.

### 3.2 Homolytic dissociation enthalpy of $RuCp_2$ and RuCpPy

Table 4 shows the homolytic dissociation enthalpies of $RuCp_2$ (R8) and RuCpPy (R9). They were computed starting from the heterolytic dissociation enthalpies (reactions R1 and R2) by subtracting the ionization energy ($IE_{Ru}$) of ruthenium and adding the electron affinities (EA) of the relevant ligands, Cp or Py radical (including thermal corrections, giving $\Delta H_{Cp}$ and $\Delta H_{Py}$), as described by the reaction cycles in Fig. 6. As the $IE_{Ru}$ and ligand EAs are the only quantities calculated in this work for which experimental data are available, it is worthwhile to first take a closer look at these data. Both properties are notoriously difficult to describe accurately by means of traditional wave-function-based methods, requiring extensive basis set to fully capture the difference in dynamical correlation between two systems differing by one or two electrons. As to be expected, CASPT2 overestimates the electron affinities of both radicals, while underestimating the (absolute) value of the Ru ionization energy. The errors are, however, quite acceptable, 3 kcal/mol or less. The CASPT2 error on the Ru ionization energy is the sum of two errors 0.6 and 2.4 kcal/mol for the first and second ionization energies, respectively. On the other hand, less accurate results for both properties are obtained from DFT, with errors in the opposite direction. All functionals overestimate the (absolute) value of $IE_{Ru}$. The pure PBE functional suffers from an error as large as 17.7 kcal/mol. As indicated by a study of a series of 4d and 5d transition metal atoms [33], errors of this size are typical for pure GGA functionals. The B3LYP and PBE0 functionals perform better, with errors between 5 and 10 kcal/mol. The Cp and Py EAs are fairly accurately described by all considered functionals. B3LYP shows the largest deviation from experiment (around –6 kcal/mol), while PBE gives the best result (around –3 kcal/mol).

Assuming that the values obtained from CASPT2 for the heterolytic dissociation enthalpy of both molecules, 711.8 kcal/mol for $RuCp_2$ and 691.9 kcal/mol for RuCpPy (cfr Table 2), are of a similar accuracy as found in our previous work on ferrocene [8, 18] (i.e., within the experimental uncertainty of ±6 kcal/mol for that molecule), an accurate estimate of the homolytic dissociation enthalpies of both molecules considered here should be obtained by combining those values with the experimental data of $IE_{Ru}$, $\Delta H_{Cp}$, and $\Delta H_{Py}$. These estimates are 241.0 kcal/mol for $RuCp_2$ and 227.9 kcal/mol for RuCpPy. The difference between both values is reduced by 7.0 kcal/mol with respect to the difference in heterolytic dissociation enthalpies, because of the larger EA of Py as compared to Cp. As can be seen from Table 4, the combined errors on $IE_{Ru}$ and the ligand EAs add up to a total error of around +8 kcal/mol with CASPT2. While CASPT2 thus overestimates the homolytic dissociation enthalpies, the

**Table 4** $\Delta H^\circ_{298}$ (kcal/mol) of the homolytic dissociation reactions of $RuCp_2$ and RuCpPy

| | $RuCp_2 \longrightarrow Ru + 2Cp^\cdot$ (R8) | | | | $RuCpPy \longrightarrow Ru + Cp^\cdot + Py^\cdot$ (R9) | | | | |
|---|---|---|---|---|---|---|---|---|---|
| | PBE | B3LYP | PBE0 | CASPT2 | PBE | B3LYP | PBE0 | CASPT2 | Exp. |
| $\Delta H_{hetero}$ | 720.9 | 679.3 | 700.7 | 711.9 | 703.7 | 662.1 | 682.5 | 691.9 | |
| $-IE_{Ru}$ | −573.9 | −565.9 | −561.1 | −553.3 | −573.9 | −565.9 | −561.1 | −553.3 | −556.2[b] |
| $\Delta H_{Cp}$ | 39.9 | 36.9 | 38.0 | 45.4[a] | 39.9 | 36.9 | 38.0 | 45.4[a] | 42.7[a,c] |
| $\Delta H_{Py}$ | | | | | 46.6 | 43.9 | 44.6 | 51.6[a] | 49.6[a,c] |
| $\Delta H_{homo}$ | 226.8 | 187.2 | 215.5 | 249.3 | 216.1 | 177.0 | 204.0 | 235.6 | |

[a] ZPE and thermal correction to the enthalpy were taken from PBE0 result

[b] Ref. [29, 30]

[c] Electron affinity (*EA*) of the cyclopentadienyl radical (41.69 ± 0.14 kcal/mol) from Ref. [31] and of the pyrrolyl radical (49.47 ± 0.23 kcal/mol) from Ref. [32]. $\Delta H_{Cp}$ and $\Delta H_{Py}$ are defined as the enthalpy difference for the reactions $Cp^- \longrightarrow Cp^\cdot + e^-$ and $Py^- \longrightarrow Py^\cdot + e^-$, see Fig. 6

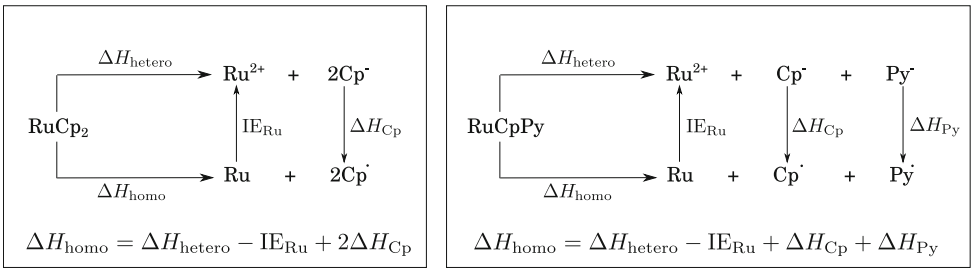


**Fig. 6** Reaction cycle for computing the homolytic dissociation enthalpy of $RuCp_2$ and RuCpPy

corresponding DFT errors are negative but more severe. The ordering of the homolytic dissociation energies with respect to the different functionals, PBE > PBE0 > B3LYP, remains the same as for the heterolytic dissociation energies, but all three functionals now underbind. As for the heterolytic dissociation energies, the "best" results are still obtained with PBE, with an error of −12 to −14 kcal/mol, while the largest errors are found with B3LYP, −54 to −58 kcal/mol. However, more importantly, in view of our aim to study the relative performance of these and other Ru compounds in ALD experiments, the difference in the homolytic dissociation enthalpies between both molecules is very similar for the three functionals, 10–11 kcal/mol, and also lies within 3 kcal/mol of the difference 13.1 kcal/mol obtained as our "best estimate" (i.e., making use of experimental data for the IE and EA), while CASPT2 gives 13.7 kcal/mol.

## 4 Conclusions

The calculated heterolytic dissociation enthalpies of $RuCp_2$ and RuCpPy show that both molecules are very stable, since their binding energies are very high. This is in agreement with the high thermal stability of these precursors, allowing ALD up to temperatures as high as 350–400 °C [4, 5]. RuCpPy is about 20 kcal/mol less stable than ruthenocene with respect to heterolytic dissociation and 13 kcal/mol with respect to homolytic dissociation. This could at least partly explain the higher reactivity of RuCpPy in ALD experiments. However, other factors, such as the adsorption energy at the surface and structural changes during adsorption affecting the possibility of dissociation, may of course play an equally or even more important role. Therefore, we are currently also investigating the chemisorption reactions of $RuCp_2$ and RuCpPy at different surfaces. For this purpose, we make use of DFT with periodic boundary conditions. The present study therefore also serves as a benchmarking study for the quality of different DFT functionals, with PBE in particular, as this functional will be used in the solid-state calculations. To test the quality of the different functionals, high-level CASPT2 calculations with extensive basis sets were employed. From the comparison between the DFT results and CASPT2, we find that, although the absolute dissociation energies obtained from DFT may be afflicted with very large errors (up to more than 50 kcal/mol with B3LYP), the differences between both molecules, both for the heterolytic and homolytic dissociation enthalpies, are well-described. This is of course due to a large cancellation of errors of the absolute dissociation enthalphies of both molecules. The calculations also indicate that, of the three functionals studied, PBE performs best as compared to CASPT2. This is, however, a conclusion that we believe is not extendable to other (e.g., first-row metallocene) systems.

**Acknowledgments** This investigation has been supported by grants from the Flemish Science Foundation (FWO) and from the Concerted Research Action of the Flemish Government (GOA).

## References

1. George SM (2010) Chem Rev 110:111
2. Knez M, Nielsch K, Niinistö L (2007) Adv Mater 19:3425
3. Bohr M, Chau R, Ghani T, Mistry K (2007) Spectrum, IEEE 44:29
4. Aaltonen T, Alén P, Ritala M, Leskelä M (2003) Chem Vap Deposition 9:45
5. Kukli K, Kemell M, Puukilainen E, Aarik J, Aidla A, Sajavaara T, Laitinen M, Tallarida M, Sundqvist J, Ritala M, Leskelä M (2011) J Electrochem Soc 158:D158
6. Swerts J, Salimullah MM, Popovici M, Kim MS, Pawlak MA, Delabie A, Schaekers M, Tomida K, Kaczer B, Opsomer K, Vrancken C, Debusschere I, Altimime L, Kittl JA, Van Elshocht S (2011) ECS Trans 41:41
7. Elliott SD (2010) Langmuir 26:9179
8. Phung QM, Vancoillie S, Pierloot K (2012). J Chem Theory Comput 8:883
9. Ahlrichs R, Bär M, Häser M, Horn H, Kälmel C (1989) Chem Phys Lett 162:165
10. Aquilante F, De Vico L, Ferré N, Ghigo G, Malmqvist PÅ, Neogrády P, Pedersen TB, Pitoňák M, Reiher M, Roos BO, Serrano-Andrés L, Urban M, Veryazov V, Lindh R (2010) J Comput Chem 31:224
11. Weigend F, Furche F, Ahlrichs R (2003) J Chem Phys 119:12753
12. Weigend F, Häser M, Patzelt H, Ahlrichs R (1998) Chem Phys Lett 294:143
13. Andrae D, Häußermann U, Dolg M, Stoll H, Preuß H (1990) Theoretica Chimica Acta 77:123
14. Grimme S (2006) J Comput Chem 27:1787

15. Roos BO, Lindh R, Malmqvist PÅ, Veryazov V, Widmark PO (2005) J Phys Chem A 109:6575
16. Roos BO, Lindh R, Malmqvist PÅ, Veryazov V, Widmark PO (2004) J Phys Chem A 108:2851
17. Widmark PO, Malmqvist PÅ, Roos BO (1990) Theor Chem Acc 77:291
18. Vancoillie S, Zhao H, Tran VT, Hendrickx MFA, Pierloot K (2011) J Chem Theory Comput 7:3961
19. Aquilante F, Malmqvist PÅ, Pedersen TB, Ghosh A, Roos BO (2008) J Chem Theory Comput 4:694
20. Hess BA (1986) Phys Rev A 33:3742
21. Reiher M, Wolf A (2004) J Chem Phys 121:2037
22. Reiher M, Wolf A (2004) J Chem Phys 121:10945
23. Ghigo G, Roos BO, Malmqvist PÅ (2004) Chem Phys Lett 396:142
24. Forsberg N, Malmqvist PÅ (1997) Chem Phys Lett 274:196
25. Pierloot K, Vancoillie S (2006) J Chem Phys 125:124303
26. Pierloot K (2001) In: Cundari TR (ed.) Computational organometallic chemistry, pp 123–158. Marcel Dekker, Inc., New York
27. Seiler P, Dunitz JD (1980) Acta Crystallogr Sect B 36:2946
28. Waller MP, Braun H, Hojdis N, Bühl M (2007) J Chem Theory Comput 3:2234
29. Callender CL, Hackett PA, Rayner DM (1988) J Opt Soc Am B 5:614
30. Shenstone AG, Meggers WF (1958) J Res Natl Bur Stand (US) 61:373
31. Ichino T, Wren SW, Vogelhuber KM, Gianola AJ, Lineberger WC, Stanton JF (2008) J Chem Phys 129:084310
32. Gianola AJ, Ichino T, Hoenigman RL, Kato S, Bierbaum VM, Lineberger WC (2004) J Phys Chem A 108:10326
33. Wu Z, Kawazoe Y (2006) Chem Phys Lett 423:81